Agonist-independent Prostaglandin EP3 Receptor signaling is required to prevent insulin hypersecretion and metabolic dysfunction in a non-obese mouse model of insulin resistance

Austin Reuter[1,2,†], Jaclyn A. Wisinski[1,2,†,#], Darby C. Peter[1,2], Michael D. Schaid[1,2], Rachel J. Fenske[1,3], and Michelle E. Kimple[1,2,3,4*]

From the [1]Research Service, William S. Middleton Memorial VA Hospital, Madison, WI, 53705 and [2]Department of Medicine, Division of Endocrinology, Diabetes, and Metabolism, [3]Interdepartmental Graduate Program in Nutritional Sciences, and [4]Department of Cell and Regenerative Biology, University of Wisconsin-Madison, Madison, WI, 53705

Running Title: Effects of EP3/Gα_z signaling on beta-cell compensation

[†] These authors contributed equally to this work

[#] Present address: 3031 Cowley Hall, University of Wisconsin-Lacrosse, Lacrosse, WI 54601

* To whom correspondence should be addressed:
Michelle E. Kimple, PhD
4148 UW Medical Foundation Centennial Building
1685 Highland Avenue
Madison, WI 53705
Tel: 608-265-5627
E-mail: mkimple@medicine.wisc.edu

Keywords: animal model; beta cell (β-cell); insulin secretion; insulin resistance; G protein-coupled receptor; pancreatic islet; signal transduction; type 2 diabetes

Abstract

By 10 weeks of age, type 2 diabetes (T2D) is fully penetrant in male and female Black and Tan Brachyury (BTBR) mice homozygous for the *Leptin*^{Ob} mutation (BTBR-Ob). Pancreatic islets isolated from T2D BTBR-Ob mice and human organ donors express significantly more EP3 than those of non-diabetic controls, in addition to producing significantly more prostaglandin E_2, the most abundant and bioactive natural EP3 ligand. Treating these islets with an EP3-specific antagonist significantly elevates their glucose-stimulated and incretin-potentiated insulin secretion response. In this work, we characterize the effect of global EP3 loss on the *in vivo* metabolic and *ex vivo* islet phenotype of BTBR mice, both lean and *Leptin*^{Ob}. EP3-null BTBR-Ob mice were not protected from T2D, with fasting hyperglycemia, glucose intolerance, and insulin resistance just as severe as wild-type (WT) BTBR-Ob controls. More surprising, though, was the early and substantial development of insulin resistance and glucose intolerance in EP3-null BTBR-lean mice as compared to WT lean controls. This *in vivo* phenotype was associated with essentially uncontrolled islet insulin hypersecretion *ex vivo*. Selective up-regulation of constitutively-active EP3 splice variants in BTBR islets provides a potential mechanism by which chronic loss of a critical check on insulin secretion exacerbates peripheral insulin resistance and glucose intolerance, particularly in the context of underlying genetic defects in insulin sensitivity.

Introduction

Type 2 diabetes (T2D) occurs after a failure of the insulin-secreting pancreatic beta-cells to compensate for peripheral insulin resistance and its often-associated glucolipotoxic and inflammatory conditions. Genetically-encoded defects in beta-cell function or the ability of beta-cells to proliferate and survive can be factors in an individual's susceptibility to the disease. As a strain characteristic, Black and Tan Brachyury (BTBR) mice are more insulin resistant than the more commonly used C57BL/6J sub-strain(1), but their T2D pathogenesis when homozygous for the *Leptin*^{Ob} mutation (BTBR-Ob) is beta-cell centric. The BTBR strain has an underlying deficit in insulin granule exocytosis(2,3), and BTBR-Ob mice fail to up-regulate an islet cell cycle gene module necessary to mount a compensatory increase in beta-cell mass (4,5). Male and female BTBR-Ob mice rapidly and reproducibly develop severe obesity and insulin resistance, succumbing to T2D by 10 weeks of age(1). This makes the BTBR mouse an excellent model mimic the natural course of T2D development in susceptible individuals.

The second messenger molecule, cyclic AMP (cAMP), has been well-characterized as a potentiator of glucose-stimulated insulin secretion (GSIS) and beta-cell replication. One of the most well-characterized beta-cell signal transduction pathways is mediated by the G_s-coupled glucagon-like peptide 1 receptor (GLP-1R), a receptor for the incretin hormone, GLP-1(6,7). BTBR-Ob islets have a blunted ability to respond to GLP1R agonists (GLP1-RAs), suggesting a blockade in the cAMP production and/or cAMP signaling pathway(8,9). Prostaglandin EP3 receptor (EP3) is a G_i-coupled receptor for prostaglandin E_2 (PGE_2): its most abundant natural ligand. When EP3 is active, adenylyl cyclase activity is inhibited and cAMP production is reduced(10-14). Islets isolated from BTBR-Ob mice and T2D human organ donors produce more

PGE_2 and express more EP3 than those of non-diabetic controls and respond more strongly to glucose and GLP1-RAs when co-treated with an EP3 antagonist (8,9,13,14). EP3 antagonists have also been shown to reduce mouse and human beta-cell proliferation. Because of these findings, elevated beta-cell EP3 signaling has been proposed as a dysfunctional consequence of the T2D condition itself that could be therapeutically targeted in vivo. Arguing against this concept are studies finding global EP3 loss magnifies the development of obesity, insulin resistance, and/or glucose intolerance of aging or after moderate-fat- or high-fat-diet feeding(15-17).

In this work, we characterized the *in vivo* metabolic and *ex vivo* islet phenotype of wild-type and EP3-null BTBR-Ob mice: a model used previously to confirm the key role of PGE_2 production and EP3 expression in the beta-cell dysfunction of T2D (8,9,18,19). Unexpected findings in the BTBR-lean background provide a new dimension to our understanding of EP3 as a critical brake on insulin secretion.

Materials & Methods

Materials and Reagents

Sodium chloride (S9888), potassium chloride (P3911), magnesium sulfate heptahydrate (M9397), potassium phosphate monobasic (P0662), sodium bicarbonate (S6014), HEPES (H3375), calcium chloride dehydrate (C3881), exendin-4 (E7144) and RIA-grade bovine serum albumin (A7888) were purchased from Sigma Aldrich (St. Louis, MO, USA). Anti-insulin antibodies (Insulin + Proinsulin Antibody, 10R-I136a; Insulin + Proinsulin Antibody, biotinylated, 61E-I136bBT) were from Fitzgerald Industries (Acton, MA, USA). The 10 ng/ml insulin standard (8013-K) and assay

buffer (AB-PHK) were from Millipore. RPMI 1640 medium (11879–020: no glucose), penicillin/streptomycin (15070–063), and fetal bovine serum (12306C: qualified, heat inactivated, USDA-approved regions) were from Life Technologies (Carlsbad, CA, USA). Dextrose (D14–500) was from Fisher Scientific (Waltham, MA). Humulin R® was from Eli Lilly and Co. Guinea pig anti-insulin, antibody diluent with background reduction, EnVision™ diaminobenzidine (DAB) reagents, and and serum-free blocking agent were from Dako. Superfrost® Plus microscope slides were from Fisher Scientific (Hampton, NH, USA), and fluorescence quality 1.5-mm coverslips were from Corning Life Sciences (Lowell, MA, USA). The rat/mouse insulin ELISA kit was from Crystal Chem Inc. (Downers Grove, IL, USA). Glucose Oxidase Reagent was from Pierce. The RNeasy Mini Kit and RNase-free DNase set were from Qiagen. High-Capacity cDNA Reverse Transcription Kit was from Applied Biosystems. FastStart Universal SYBR Green Master mix was from Roche.

Mouse husbandry

Breeding colonies were housed in a limited-access, pathogen-free breeding core facility where all cages, enrichment, and water were sterilized before use on a 12-hour light/12-hour dark cycle with *ad libitum* access to water and irradiated breeder chow (Teklad 2919, Envigo). Upon weaning, mice were housed four or fewer per cage of mixed genotypes with ad libitum access to lower-fat chow in the Madison VA Animal Resource Facility (LabDiet 5001, nonirradiated). All procedures were performed according to approved protocols in accordance with the principles and guidelines established by the University of Wisconsin and Madison VA Institutional Animal Care and Use Committees. Both male and female mice were used in these experiments, as, at the age range

selected, the only statistically-significant change in metabolic parameters-of-interest was a slightly lower body weight in 8-week-old female mice as compared to male (data not shown).

Mouse metabolic phenotyping and tissue collection

Oral glucose tolerance tests (OGTTs) were performed at 6 weeks of age after a 4-6 h fast in clean cages. 1 g/kg sterile dextrose solution was administered via gavage needle at 6 weeks of age, with blood glucose levels recorded at various timepoints by blood glucose meter (AlphaTRAK) and rat/mouse–specific test strips reading of a blood droplet obtained via tail nick, as previously described(9,13,20). Insulin tolerance tests (ITTs) were performed similarly to OGTTs, except that 0.75 mg/kg Humulin-R was IP injected. To isolate pancreatic islets, mice were anesthetized by 2,2,2 tribromoethanol until unresponsive, exsanguinated by cutting the descending aorta, and the bile duct ligated and cannulated, followed by injection of ice-cold collagenase solution to inflate the pancreas as described previously(21). For terminal blood collection in order to generate plasma samples, mice were fasted 4-6 h in clean cages and anesthetized by 2,2,2 tribromoethanol until unresponsive, and mice were exsanguinated by retro-orbital puncture with an EDTA-coated microcapillary tube, followed by secondary euthanasia by cervical dislocation. Whole pancreases were harvested upon necropsy and fixed in formalin at 4 degrees C overnight, and then cryo-preserved.

Pancreas section histochemical staining and insulin immunohistochemistry

Insulin immunohistochemistry with hematoxylin counterstain (for measurement of beta-cell fractional area) was performed as previously described for paraffin-embedded pancreas sections (11,13,22). Adipose tissue and kidney were harvested upon necropsy and flash-frozen in liquid

nitrogen for future isolation of total RNA. GSIS assays were performed using a single-islet microplate GSIS assay, and total islet insulin content and secreted insulin quantified via an in-house sandwich ELISA as previously described(23).

Plasma insulin, glucose, and PGE metabolite measurements

The insulin concentration of 4-6 h fasting plasma samples and plasma samples from OGTTs was determined using a Crystal Chem high-sensitivity insulin ELISA as previously described(22). Plasma glucose was recorded via Pierce glucose oxidase assay according to the manufacturers' directions. Plasma PGE metabolite concentrations were determined by PGE metabolite EIA according to the manufacturer's protocol, as previously described(8,9).

Quantitative PCR assays

150-200 islets from each mouse islet preparation were washed with PBS and used to generate RNA samples via Qiagen RNeasy Mini Kit according to the manufacturer's protocol. Copy DNA (cDNA) was generated and relative qPCR performed via SYBR Green assay using primers validated to provide linear results upon increasing concentrations of cDNA template, as previously described(22). A list of qPCR primer sequences can be found in Table 1.

Statistical analysis

Data are expressed as mean ± standard error of the mean (SEM) unless otherwise noted. Data were analyzed as appropriate for the experimental design and as indicated in the text and figure legends. P-values < 0.05 were considered statistically significant. Statistical analyses were performed with GraphPad Prism version 7 (GraphPad Software, San Diego, CA).

Results

Mouse model generation and validation

C57BL/6J mice in which Cre expression is driven by the rat insulin promoter (RIP-Cre^{Herr}: "InsPr-Cre" in (24)) were obtained from Pedro Herrera as described previously (22). As compared to other constitutive RIP-Cre driver lines, RIP-Cre^{Herr} has low hypothalamic Cre expression (25) and does not contain the human growth hormone minigene, which has been shown in previous studies to produce full-length, active hGH that artificially enhances mouse beta-cell proliferation through the prolactin receptor(26).

B6/129 mice in which the first coding exon of the *Ptger3* gene is flanked by LoxP sites (EP3-floxed) were obtained from The Jackson Laboratory (*Ptger3*^{tm1Csml}; stock 008349, deposited by Michael Lazarus). These mice were crossed with RIP-Cre^{Herr} from our in-house colony to generate a mixed-background EP3-flox-RIP-Cre mouse, which was back-crossed into the BTBR *T+ Itpr3*^{tf}/J (BTBR) background more than 10 generations. Upon genotyping to identify experimental animals, when the floxed allele was detected, it was only the deleted allele, independent of Cre expression, meaning Cre recombination must have occurred in a germline cell early in the backcross (**Figure 1A**) (See **Table 2** for PCR primer sequences). Adipose and kidney have high EP3 expression, and no *Ptger3* amplification was detected in cDNA samples from these tissues in EP3-null BTBR-lean or BTBR-Ob mice (**Figure 1B,C**). Mouse islets, on the other hand, have relatively low EP3 expression, except when T2D (8). When islets were isolated from mice of all four groups, *Ptger3* expression in WT BTBR-Ob islet cDNA was 50-100-fold enhanced above the

low level observed in WT BTBR-lean: a finding that was ablated with the EP3-null mutation (**Figure 1D**).

Full-body EP3 loss enhances insulin resistance and promotes glucose intolerance in lean mice

By 10 weeks of age, the T2D phenotype of male and female BTBR-Ob mice is fully penetrant (1). In order to determine the effect of EP3 loss on the development of T2D, weights and random-fed blood glucose levels of BTBR-lean and -Ob mice were tracked from 4-9 weeks of age, with OGTTs planned at 6 weeks of age and ITTs planned at 8 weeks of age. BTBR-Ob mice were significantly heavier than BTBR-lean mice at all ages, as expected, with no difference by genotype (**Figure 2A**). Random-fed blood glucose levels were similarly elevated in BTBR-Ob mice as compared to BTBR-lean at all ages, again, with no difference by genotype (**Figure 2B**). As all BTBR-Ob mice were clearly T2D when OGTTs and ITTs were planned, these tests were not performed. 8-week-old WT and EP3-null BTBR-Ob mice were fasted for 4-6 h, though, and all mice had blood glucose levels over 300 mg/dl, with no difference by genotype (**Figure 2C**).

At 6 weeks of age, there was no statistically-significant difference in the mean 4-6 h fasting blood glucose level of WT and EP3-null BTBR-lean mice by genotype (**Figure 2D**). EP3-null BTBR-lean mice had significantly poorer glucose tolerance than WT controls, though, whether represented as blood glucose excursion after glucose challenge or as OGTT glucose area-under-the-curve (AUC) (**Figure 2E,F)**. At 8 weeks of age, there was still no difference in the mean 4-6 h fasting blood glucose levels between WT and EP3-null BTBR lean mice (**Figure 2G**), but, when given an insulin challenge, EP3-null BTBR-lean mice were significantly less insulin sensitive than

WT controls, whether represented as the glucose excursion from baseline or as AUC (**Figure 2H,I**).

Full-body EP3 loss has no effect on markers of beta-cell replication in BTBR-lean or -Ob islets and pancreas sections. At 9-10 weeks of age, pancreases were collected from wild-type and EP3-null BTBR-lean and BTBR-Ob mice and fixed for paraffin-embedding and sectioning. Insulin IHC was performed on pancreas sections counterstained with hematoxylin (see representative images in **Figure 3A**). Although the mean insulin-positive area of BTBR-Ob pancreas sections as compared to lean was approximately 2-fold elevated, this difference was not statistically significant, and did not differ by genotype (**Figure 3B**). Cyclin D1 (gene symbol: *Ccnd1*) is required for cell cycle progression through the G1 phase, and its expression is up-regulated at the mRNA level in actively-replicating beta-cells (27). Quantitative PCR using *Ccnd1*-specific revealed no significant differences in islet cyclin D1 mRNA abundance among the groups, whether by $Leptin^{Ob}$ or EP3-null mutational status (**Figure 3C**).

EP3 loss promotes unregulated glucose-stimulated insulin secretion in BTBR-Ob islets.

Islets were isolated from WT and EP3-null BTBR-lean and BTBR-Ob mice in order to quantify the effect of EP3 loss on beta-cell function. Glucose-stimulated insulin secretion (GSIS) assays were performed in 2.8 mM glucose or 16.7 mM glucose, the latter with or without the addition of 10 nM exendin-4 (Ex-4), a GLP1-RA. The most striking findings from these assays was the complete loss of regulated insulin secretion in islets from EP3-null BTBR-lean mice, with nearly equivalent levels of insulin secreted as a percent of content in basal or stimulatory glucose (**Figure 4A,B**). EP3-null BTBR-lean islets did have a stronger response to Ex-4 than WT controls, but this

trend was not statistically-significant and was actually reversed in EP3-null BTBR-Ob islets as compared to WT (**Figure 4A**). Finally, BTBR-Ob islets had significantly lower content than BTBR-lean islets, but, in both cases, islets from EP3-null mice had lower content than those from WT mice (**Figure 4C**).

Mouse islet EP3 mRNA expression is correlated with insulin resistance and T2D status: differential expression of the constitutively-active EP3γ variant in the BTBR strain. Three mouse EP3 splice variants exist, EP3α, EP3β, and EP3γ, differing only in the sequence of their C-terminal tails (12). Using primers common to all three splice variants, EP3 expression is about 6-fold- and 350-fold upregulated in islets from BTBR-lean and -Ob mice, respectively, as compared to those from C57BL/6J (B6) (**Figure 5A**). All three spice variants are up-regulated in BTBR-Ob as compared to B6 (~2000-fold, 20-fold, and 350-fold, for EP3α, EP3β, and EP3γ, respectively), but only EP3α and EP3γ are up-regulated in BTBR-lean as compared to B6 (~12-fold and 36-fold, respectively) (**Figure 5A**). Notably, EP3β is the only splice variant that requires PGE_2 binding in order to be active: EP3α is about 50% constitutively active and EP3γ is about 80% constitutively active (14,28,29). Islets were isolated from B6, BTBR-lean, BTBR-Ob, and EP3-null BTBR-Ob mice and used in GSIS assays in 16.7 mM glucose, with and without the addition of 10 nM sulprostone, an EP3-selecitve agonist. Only BTBR-Ob islets responded to sulprostone to reduce GSIS: an approximately 50% reduction in GSIS that was lost when islets were isolated from EP3-null BTBR-Ob mice (**Figure 5B**).

Discussion

We and others have previously proposed elevated islet PGE_2 production and EP3 expression as a dysfunctional response to the T2D condition, actively contributing to the loss of functional beta-cell mass(8,9,12,18,27,30-33). Yet, EP3 loss did not protect BTBR-Ob mice from T2D, even in the context of a similar full-body metabolic phenotype as WT BTBR-Ob mice. One of the defects in the BTBR-Ob line is a failure to up-regulate beta-cell replication in response to severe obesity and insulin resistance necessary to mount a compensatory increase in beta-cell mass(4,5). Although we did not directly measure beta-cell mass in this study, insulin-positive pancreas area served as a surrogate, and was no different among the groups. Combined with a lack of up-regulation of cyclin D1 mRNA expression in islets from EP3-null BTBR-Ob mice as compared to WT controls, it is likely EP3 loss is not enough to overcome this genetically-encoded defect in replication. Much more interesting in our minds, though, was the unexpected phenotype of EP3-null mice in the BTBR-lean background.

Three previous studies have metabolically phenotyped C57BL/6J EP3-null mice, and in all three of these studies, the effect of EP3 loss on worsening insulin resistance and glucose intolerance was gradual and/or required a metabolic challenge. Sanchez-Alavez and colleagues maintained wild-type and EP3-null mice on breeder chow (approximately 20 kcal% fat, as compared to 10 kcal% fat in normal rodent chow) for 40 weeks, revealing EP3-null mice gradually became heavier than wild-type controls, developing hyperinsulinemia, hyperleptinemia, and worsening glucose tolerance between 3 and 6 months of age(16). While the fat content of the diet used by Xu and colleagues was not specified, they also found mice deficient in EP3, or expressing only the EP3β splice variant, started becoming obese and insulin resistant around 20 weeks of age, a phenotype linked to unregulated adipogenesis and lipolysis (17). Ceddia and colleagues used a 16-week high-

fat-diet (HFD) regimen, initiated at 4 weeks of age, revealing a diet-dependent decrement in insulin sensitivity that was correlated with unregulated lipolysis, dyslipidemia, and systemic inflammation due to loss of EP3 in adipose tissue(15). No studies, including those by our own group, have identified any significant metabolic phenotype, whether in vivo or in islets ex vivo, after genetic ablation or pharmacological inhibition of EP3 or its signaling partners in young, lean C57BL/6J mice. The BTBR strain, on the other hand, is much more insulin resistant than C57BL/6J, whether measured by adipocyte glucose uptake or hyperinsulinemic-euglycemic clamp(1). Lean BTBR mice also have fasting hyperinsulinemia and elevated plasma C-peptide levels as compared to C57BL/6J mice(1), meaning their beta-cells are already under a great deal of stress. If one considers the underlying insulin resistance phenotype of the BTBR strain, coupled with the exacerbation of insulin resistance expected as a result of systemic loss of EP3, the rapid and significant effect of EP3 loss on BTBR-lean mouse glucose tolerance is not unexpected.

A SNP in the BTBR version of the *Stxbp5l* gene, encoding tomosyn-2, is responsible for a diabetes susceptibility QTL in an F2 intercross between the BTBR and C57BL/6J lines(2). Tomosyn-2 is a negative regulator of SNARE complex formation and insulin granule exocytosis and is normally rapidly degraded after the beta-cell is exposed to stimulatory glucose. The BTBR tomosyn-2 variant is relatively insensitive to this glucose-stimulated proteolytic degradation, significantly blunting second-phase GSIS(3). Yet, tomosyn-2 protein degradation is also promoted by cAMP-stimulated phosphorylation, among other metabolic signals. In this study, we found islet EP3 expression up-regulated in islets from BTBR-lean mice as compared to B6, with the EP3γ splice variant being the most highly up-regulated. Notably, beta-cell EP3γ couples exclusively to the unique inhibitory G protein alpha subunit, $G\alpha_z$, reducing cAMP production and GSIS with nearly

full constitutive activity, even in the absence of agonist (14). It is possible loss of EP3 and relief of a tonic EP3γ/Gα_z-mediated brake on BTBR beta-cell cAMP production compensated for an underlying secretory defect, either through the classical mechanism(s) of PKA- and Rap1-mediated recruitment of insulin granules to the plasma membrane; targeting of tomosyn-2 for degradation; or both. More studies in a model where our results will not be confounded by significant underlying differences in metabolic phenotypes will be necessary to tease apart this mechanism.

In sum, the results of the current study, combined with the published results on the impact of EP3/Gα_z loss on beta-cell function and beta-cell replication/mass in non-diabetic and T2D/glucolipotoxic mouse models supports the importance of EP3 in regulating key beta-cell signaling events that impact beta-cell biology and a divergence in these downstream signaling events depending on the physiologic conditions to which the beta-cell is exposed. The extreme insulin hypersecretion phenotype of EP3-null BTBR-lean islets underscores the key role of beta-cell EP3 as a negative regulator of GSIS, and, although only correlative at this point, suggests BTBR mouse beta-cells express higher-than-typical EP3 as a functional compensatory mechanism to reduce beta-cell stress in the context of underlying insulin resistance. Based on the clearly worsening metabolic phenotype of EP3-null BTBR-lean mice before 10 weeks of age, we expect, but cannot confirm, they ultimately would have progressed to T2D. This concept does have support in epidemiological studies in human populations with an underlying genetic defect pre-disposing to skeletal muscle insulin resistance, in which the progression to T2D is dependent on the beta-cell (34-38). Confirmation of this model is the subject of much current work.

Acknowledgements

We wish to thank the many present and former members of the Kimple Laboratory who contributed technical assistance or scientific discussion during the course of these experiments. We would particularly like to thank Audrianna Wu, a Madison Metropolitan School District high school student who completed a summer research experience in the Kimple lab and helped with pancreas slide staining. We would also like to thank Maureen Gannon and Rich Breyer at Vanderbilt University Medical Center for productive discussions regarding EP3 signaling in beta-cell function and replication. This work was supported in part by Merit Review Award I01 BX003700 from the United States (U.S.) Department of Veterans Affairs Biomedical Laboratory Research and Development Service (BLR&D) (to MEK). Further support was provided by NIH Grants K01 DK080845 (to MEK), R01 DK102598 (to MEK), and F31 DK109698 (to RJF); ADA Grant 1-16-IBS-212 (to MEK), and JDRF Grant 17-2011-608 (to MEK). The content is solely the responsibility of the authors and does not necessarily represent the official views of the National Institutes of Health, the U.S. Department of Veterans Affairs, or the United States Government. The funding bodies had no role in any aspect of the work described in this manuscript.

Author Contributions

Conceptualization, MEK; data curation, AR, JAW, and MEK; formal analysis, AR, JAW, and MEK; funding acquisition, RJF and MEK; investigation, AR, JAW, DP, MDS, and RJF; methodology, AR, JAW, and MEK; project administration, MEK; supervision, JAW and MEK; visualization, AR, JAW, and MEK; writing—original draft, AR, JAW, and MEK; writing—review and editing, MEK. All authors have read and agreed to the published version of the manuscript.

Conflict of Interest

The authors declare that they have no conflicts of interest with the contents of this article. The content is solely the responsibility of the authors and does not necessarily represent the official views of the National Institutes of Health, the U.S. Department of Veterans Affairs, or the United States Government.

References

1. Clee, S. M., Nadler, S. T., and Attie, A. D. (2005) Genetic and genomic studies of the BTBR ob/ob mouse model of type 2 diabetes. *American journal of therapeutics* **12**, 491-498
2. Bhatnagar, S., Oler, A. T., Rabaglia, M. E., Stapleton, D. S., Schueler, K. L., Truchan, N. A., Worzella, S. L., Stoehr, J. P., Clee, S. M., Yandell, B. S., Keller, M. P., Thurmond, D. C., and Attie, A. D. (2011) Positional cloning of a type 2 diabetes quantitative trait locus; tomosyn-2, a negative regulator of insulin secretion. *PLoS Genet* **7**, e1002323
3. Bhatnagar, S., Soni, M. S., Wrighton, L. S., Hebert, A. S., Zhou, A. S., Paul, P. K., Gregg, T., Rabaglia, M. E., Keller, M. P., Coon, J. J., and Attie, A. D. (2014) Phosphorylation and degradation of tomosyn-2 de-represses insulin secretion. *The Journal of biological chemistry* **289**, 25276-25286
4. Davis, D. B., Lavine, J. A., Suhonen, J. I., Krautkramer, K. A., Rabaglia, M. E., Sperger, J. M., Fernandez, L. A., Yandell, B. S., Keller, M. P., Wang, I. M., Schadt, E. E., and Attie, A. D. (2010) FoxM1 is up-regulated by obesity and stimulates beta-cell proliferation. *Molecular endocrinology* **24**, 1822-1834
5. Keller, M. P., Choi, Y., Wang, P., Davis, D. B., Rabaglia, M. E., Oler, A. T., Stapleton, D. S., Argmann, C., Schueler, K. L., Edwards, S., Steinberg, H. A., Chaibub Neto, E., Kleinhanz, R., Turner, S., Hellerstein, M. K., Schadt, E. E., Yandell, B. S., Kendziorski, C., and Attie, A. D. (2008) A gene expression network model of type 2 diabetes links cell cycle regulation in islets with diabetes susceptibility. *Genome research* **18**, 706-716
6. Drucker, D. J. (2003) Glucagon-like peptides: regulators of cell proliferation, differentiation, and apoptosis. *Molecular endocrinology* **17**, 161-171
7. Baggio, L. L., and Drucker, D. J. (2006) Therapeutic approaches to preserve islet mass in type 2 diabetes. *Annu Rev Med* **57**, 265-281
8. Kimple, M. E., Keller, M. P., Rabaglia, M. R., Pasker, R. L., Neuman, J. C., Truchan, N. A., Brar, H. K., and Attie, A. D. (2013) Prostaglandin E2 receptor, EP3, is induced in diabetic islets and negatively regulates glucose- and hormone-stimulated insulin secretion. *Diabetes* **62**, 1904-1912
9. Neuman, J. C., Schaid, M. D., Brill, A. L., Fenske, R. J., Kibbe, C. R., Fontaine, D. A., Sdao, S. M., Brar, H. K., Connors, K. M., Wienkes, H. N., Eliceiri, K. W., Merrins, M. J., Davis, D. B., and Kimple, M. E. (2017) Enriching Islet Phospholipids With Eicosapentaenoic Acid Reduces Prostaglandin E2 Signaling and Enhances Diabetic beta-Cell Function. *Diabetes* **66**, 1572-1585
10. Kimple, M. E., Nixon, A. B., Kelly, P., Bailey, C. L., Young, K. H., Fields, T. A., and Casey, P. J. (2005) A role for G(z) in pancreatic islet beta-cell biology. *The Journal of biological chemistry* **280**, 31708-31713
11. Kimple, M. E., Moss, J. B., Brar, H. K., Rosa, T. C., Truchan, N. A., Pasker, R. L., Newgard, C. B., and Casey, P. J. (2012) Deletion of GalphaZ protein protects against diet-induced glucose intolerance via expansion of beta-cell mass. *The Journal of biological chemistry* **287**, 20344-20355
12. Neuman, J. C., and Kimple, M. E. (2013) The EP3 Receptor: Exploring a New Target for Type 2 Diabetes Therapeutics. *J Endocrinol Diabetes Obes* **1**
13. Brill, A. L., Wisinski, J. A., Cadena, M. T., Thompson, M. F., Fenske, R. J., Brar, H. K., Schaid, M. D., Pasker, R. L., and Kimple, M. E. (2016) Synergy Between Galphaz

Deficiency and GLP-1 Analog Treatment in Preserving Functional beta-Cell Mass in Experimental Diabetes. *Molecular endocrinology* **30**, 543-556
14. Schaid, M. D., Green, C. L., Peter, D. C., Gallagher, S. J., Guthery, E., Carbajal, K. A., Harrington, J. M., Kelly, G. M., Reuter, A., Wehner, M. L., Brill, A. L., Neuman, J. C., Lamming, D. W., and Kimple, M. E. (2020) Agonist-independent Galphaz activity negatively regulates beta-cell compensation in a diet-induced obesity model of type 2 diabetes. *The Journal of biological chemistry*
15. Ceddia, R. P., Lee, D., Maulis, M. F., Carboneau, B. A., Threadgill, D. W., Poffenberger, G., Milne, G., Boyd, K. L., Powers, A. C., McGuinness, O. P., Gannon, M., and Breyer, R. M. (2016) The PGE2 EP3 Receptor Regulates Diet-Induced Adiposity in Male Mice. *Endocrinology* **157**, 220-232
16. Sanchez-Alavez, M., Klein, I., Brownell, S. E., Tabarean, I. V., Davis, C. N., Conti, B., and Bartfai, T. (2007) Night eating and obesity in the EP3R-deficient mouse. *Proceedings of the National Academy of Sciences of the United States of America* **104**, 3009-3014
17. Xu, H., Fu, J. L., Miao, Y. F., Wang, C. J., Han, Q. F., Li, S., Huang, S. Z., Du, S. N., Qiu, Y. X., Yang, J. C., Gustafsson, J. A., Breyer, R. M., Zheng, F., Wang, N. P., Zhang, X. Y., and Guan, Y. F. (2016) Prostaglandin E2 receptor EP3 regulates both adipogenesis and lipolysis in mouse white adipose tissue. *J Mol Cell Biol* **8**, 518-529
18. Schaid, M. D., Zhu, Y., Richardson, N. E., Patibandla, C., Ong, I. M., Fenske, R. J., Neuman, J. C., Guthery, E., Reuter, A., Sandhu, H. K., Fuller, M. H., Cox, E. D., Davis, D. B., Layden, B. T., Brasier, A. R., Lamming, D. W., Ge, Y., and Kimple, M. E. (2021) Systemic Metabolic Alterations Correlate with Islet-Level Prostaglandin E2 Production and Signaling Mechanisms That Predict beta-Cell Dysfunction in a Mouse Model of Type 2 Diabetes. *Metabolites* **11**
19. Zhu, Y., Wancewicz, B., Schaid, M., Tiambeng, T. N., Wenger, K., Jin, Y., Heyman, H., Thompson, C. J., Barsch, A., Cox, E. D., Davis, D. B., Brasier, A. R., Kimple, M. E., and Ge, Y. (2021) Ultrahigh-Resolution Mass Spectrometry-Based Platform for Plasma Metabolomics Applied to Type 2 Diabetes Research. *J Proteome Res* **20**, 463-473
20. Fenske, R. J., and Kimple, M. E. (2018) Targeting dysfunctional beta-cell signaling for the potential treatment of type 1 diabetes mellitus. *Experimental biology and medicine* **243**, 586-591
21. Neuman, J. C., Truchan, N. A., Joseph, J. W., and Kimple, M. E. (2014) A method for mouse pancreatic islet isolation and intracellular cAMP determination. *J Vis Exp*, e50374
22. Fenske, R. J., Cadena, M. T., Harenda, Q. E., Wienkes, H. N., Carbajal, K., Schaid, M. D., Laundre, E., Brill, A. L., Truchan, N. A., Brar, H., Wisinski, J., Cai, J., Graham, T. E., Engin, F., and Kimple, M. E. (2017) The Inhibitory G Protein alpha-Subunit, Galphaz, Promotes Type 1 Diabetes-Like Pathophysiology in NOD Mice. *Endocrinology* **158**, 1645-1658
23. Truchan, N. A., Brar, H. K., Gallagher, S. J., Neuman, J. C., and Kimple, M. E. (2015) A single-islet microplate assay to measure mouse and human islet insulin secretion. *Islets* **7**, e1076607
24. Herrera, P. L. (2000) Adult insulin- and glucagon-producing cells differentiate from two independent cell lineages. *Development* **127**, 2317-2322
25. Magnuson, M. A., and Osipovich, A. B. (2013) Pancreas-specific Cre driver lines and considerations for their prudent use. *Cell metabolism* **18**, 9-20

26. Oropeza, D., Jouvet, N., Budry, L., Campbell, J. E., Bouyakdan, K., Lacombe, J., Perron, G., Bergeron, V., Neuman, J. C., Brar, H. K., Fenske, R. J., Meunier, C., Sczelecki, S., Kimple, M. E., Drucker, D. J., Screaton, R. A., Poitout, V., Ferron, M., Alquier, T., and Estall, J. L. (2015) Phenotypic Characterization of MIP-CreERT1Lphi Mice With Transgene-Driven Islet Expression of Human Growth Hormone. *Diabetes* **64**, 3798-3807
27. Carboneau, B. A., Allan, J. A., Townsend, S. E., Kimple, M. E., Breyer, R. M., and Gannon, M. (2017) Opposing effects of prostaglandin E2 receptors EP3 and EP4 on mouse and human beta-cell survival and proliferation. *Molecular metabolism* **6**, 548-559
28. Irie, A., Segi, E., Sugimoto, Y., Ichikawa, A., and Negishi, M. (1994) Mouse prostaglandin E receptor EP3 subtype mediates calcium signals via Gi in cDNA-transfected Chinese hamster ovary cells. *Biochemical and biophysical research communications* **204**, 303-309
29. Irie, A., Sugimoto, Y., Namba, T., Harazono, A., Honda, A., Watabe, A., Negishi, M., Narumiya, S., and Ichikawa, A. (1993) Third isoform of the prostaglandin-E-receptor EP3 subtype with different C-terminal tail coupling to both stimulation and inhibition of adenylate cyclase. *Eur J Biochem* **217**, 313-318
30. Neuman, J. C., Fenske, R. J., and Kimple, M. E. (2017) Dietary polyunsaturated fatty acids and their metabolites: Implications for diabetes pathophysiology, prevention, and treatment. *Nutrition and healthy aging* **4**, 127-140
31. Robertson, R. P. (2017) The COX-2/PGE2/EP3/Gi/o/cAMP/GSIS Pathway in the Islet: The Beat Goes On. *Diabetes* **66**, 1464-1466
32. Schaid, M. D., Wisinski, J. A., and Kimple, M. E. (2017) The EP3 Receptor/Gz Signaling Axis as a Therapeutic Target for Diabetes and Cardiovascular Disease. *The AAPS journal* **19**, 1276-1283
33. Abdel-Magid, A. F. (2015) Prostaglandin EP3 Receptor Antagonists May Provide Novel Treatment for Diabetes. *ACS medicinal chemistry letters* **6**, 626-627
34. Lillioja, S., and Bogardus, C. (1988) Obesity and insulin resistance: lessons learned from the Pima Indians. *Diabetes Metab Rev* **4**, 517-540
35. Ling, C., Poulsen, P., Carlsson, E., Ridderstrale, M., Almgren, P., Wojtaszewski, J., Beck-Nielsen, H., Groop, L., and Vaag, A. (2004) Multiple environmental and genetic factors influence skeletal muscle PGC-1alpha and PGC-1beta gene expression in twins. *The Journal of clinical investigation* **114**, 1518-1526
36. Maeda, R., Raz, I., Zurlo, F., and Sommercorn, J. (1991) Activation of skeletal muscle casein kinase II by insulin is not diminished in subjects with insulin resistance. *The Journal of clinical investigation* **87**, 1017-1022
37. Poulsen, P., Wojtaszewski, J. F., Petersen, I., Christensen, K., Richter, E. A., Beck-Nielsen, H., and Vaag, A. (2005) Impact of genetic versus environmental factors on the control of muscle glycogen synthase activation in twins. *Diabetes* **54**, 1289-1296
38. DeFronzo, R. A., and Tripathy, D. (2009) Skeletal muscle insulin resistance is the primary defect in type 2 diabetes. *Diabetes Care* **32 Suppl 2**, S157-163

Table 1: Quantitative PCR (qPCR) Primer Sequences

Protein	Gene Symbol	Primer Sequences	Species Selectivity
Prostaglandin EP3 receptor (EP3)	*Ptger3*	F: GCTATCCCGCAGCTGAG R: CGCAGTCGTCGGTAGTAC	mouse
EP3α splice variant		F: GCTTCAGCTCCACCTCCTT R: CATCATCTTTCCAGCTGGTCACT	mouse
EP3β splice variant		F: GGAAGTTCTGCCAGATGATGAA R: ATTCTCAGACCCAGGGAAACA	mouse
EP3γ splice variant		F: AGTTCTGCCAGGTAGCAAACG R: GCCTGCCCTTTCTGTCCAT	mouse
Cyclin D1	*Ccnd1*	F: CTGACACCAATCTCCTCAACGAC R: GCGGCCAGGTTCCACTTGAGC	mouse
β-actin	*Actb*	F: TCTTGGGTATGGAATCCTGTGGCA R: TCTCCTTCTGCATCCTGTCAGCAA	mouse

Table 2: Primer Sequences and expected PCR product sizes for genotyping RIP-Cre-EP3-null and RIP-Cre-Gα_z-null lean and *Leptin*^{Ob} mice

Reaction	Primer Sequences	Band Size	allele
EP3-floxed	F: TCAACCTGCTAATCCCGCTG	424	deleted
	R: CAGTACCCGGCTTCTTAGGG	304	floxed
	ΔF: ACGTAACCCAAAGGCTGATGAG	194	wild-type
Cre Transgene	F: TGGTTTCCCGCAGAACCTGAAG	220	carrier
	R: GAGCCTGTTTTGCACGTTCACC	none	non-carrier
***Lep*^{Ob} mut.**	F: GGGCTTCACCCCATTCTGAG	104,44,14	mutant
	R: GGGAGCAGCTCTTGGAGAAG	144,14	wild-type

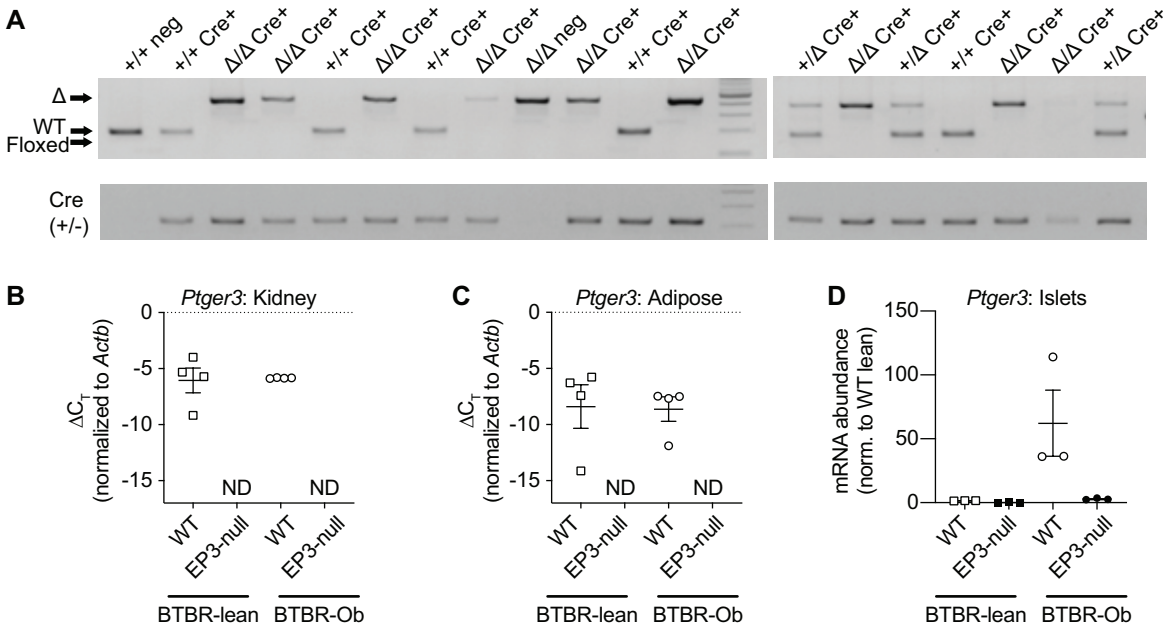

Figure 1. Germline transmission of the EP3-floxed deleted allele created a full-body EP3-null BTBR-lean and BTBR-Ob mouse. A: Genotyping results from ear punches showing only the wild-type or deleted allele, and not the floxed allele, in all genotyping reactions, regardless of Cre expression. B,C: Quantitative PCR (qPCR) cycle time (C_T) as normalized to β-actin (*Bact*) (ΔC_T) using primers amplifying all three mouse EP3 splice variants in (B) kidney and (C) adipose tissue. ND = not detected. D: Islet *Ptger3* mRNA abundance, as calculated via the $2^{\Delta\Delta C_T}$ method, normalized to the mean ΔC_T of WT lean.

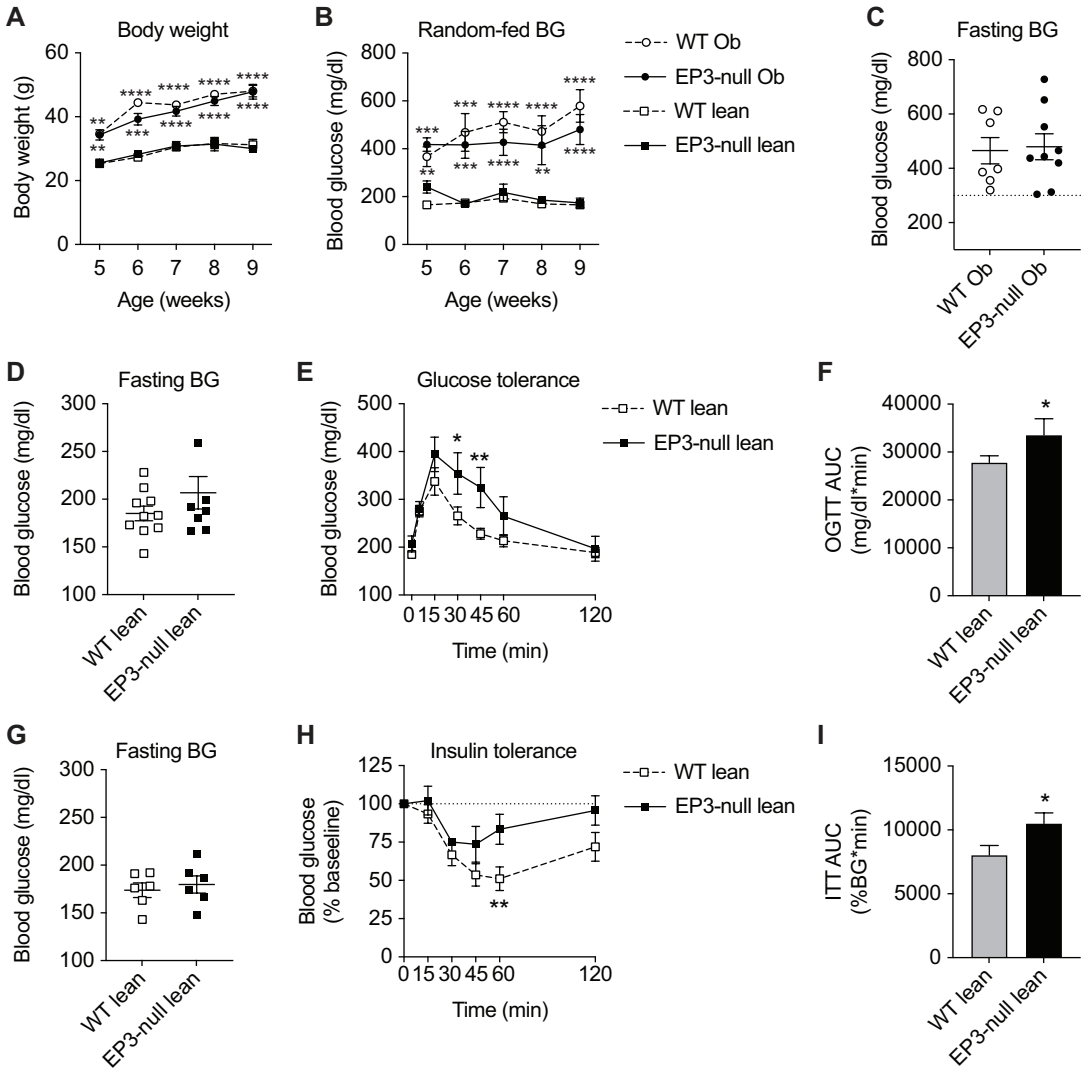

Figure 2: Full-body EP3 loss has no impact on the early metabolic phenotype of BTBR-Ob mice but worsens insulin resistance and causes glucose intolerance in BTBR-lean mice. A,B: (A) Body weights (B) and random-fed blood glucose levels of 5-9-week old WT and EP3-null BTBR-lean and -Ob mice. N=9-14 mice/group. C: 4-6 h fasting blood glucose levels of 8-week-old WT and EP3-null BTBR-Ob mice. Mice with fasting blood glucose levels at or above 300 mg/dl (dashed line) were defined as hyperglycemic. N=7-9 mice/group. D-F: (D) 4-6 h fasting blood glucose levels, (E) glucose excursions after 1 g/kg oral glucose challenge, and (F) and oral glucose tolerance test (OGTT) area-under-the-curve (AUC) analysis of 6-week-old WT and EP3-null BTBR-lean mice. N=7-10 mice/group. G-I: (G) 4-6 h fasting blood glucose levels, (H) glucose excursions after ip insulin administration (normalized to baseline blood glucose), and (I) and insulin tolerance test (ITT) area-under-the-curve (AUC) analysis 8-week-old WT and EP3-null BTBR-lean mice. N=6 mice/group. In C, D, F, G, and I, data were compared by two-way t-test. In A, B, E, and H, data were compared by two-way paired ANOVA with Holm-Sidak test post-hoc to correct for multiple comparisons. *, $p < 0.05$, **, $p < 0.01$, ***, $p < 0.001$, and ****, $p < 0.0001$ vs. WT lean. If a comparison is not shown, the difference between the means was not statistically-significant.

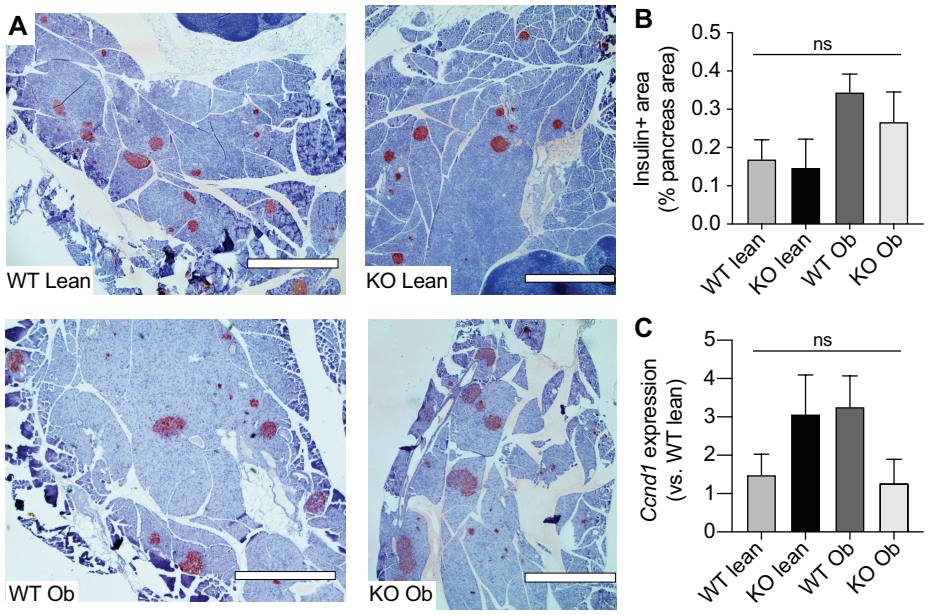

Figure 3: Beta-cell fractional area and islet cyclin D1 expression are unaffected by EP3 loss in samples from both BTBR-lean and BTBR-Ob mice. A,B: Paraffin-embedded, fixed pancreas sections from 9-10-week old wild-type and EP3-null BTBR-Ob mice were subject to insulin immunohistochemical staining, followed by hematoxylin counter-staining in order to quantify insulin-positive pancreas area as a function of total pancreas area. (A) Representative images from wild-type (WT) BTBR-lean, WT BTBR-Ob, EP3-null (KO) BTBR-lean, and KO BTBR-Ob. (B) Quantification of insulin-positive pancreas area. C: Cyclin D1 (Gene symbol: *Ccnd1*) mRNA abundance in cDNA samples from WT or EP3-null BTBR-lean and -Ob mice as quantified by qCPR. In (B) and (C), N=3-5 independent observations per group, and data were compared by one-way ANOVA with Holm-Sidak test post-hoc to correct for multiple comparisons. ns = not significant.

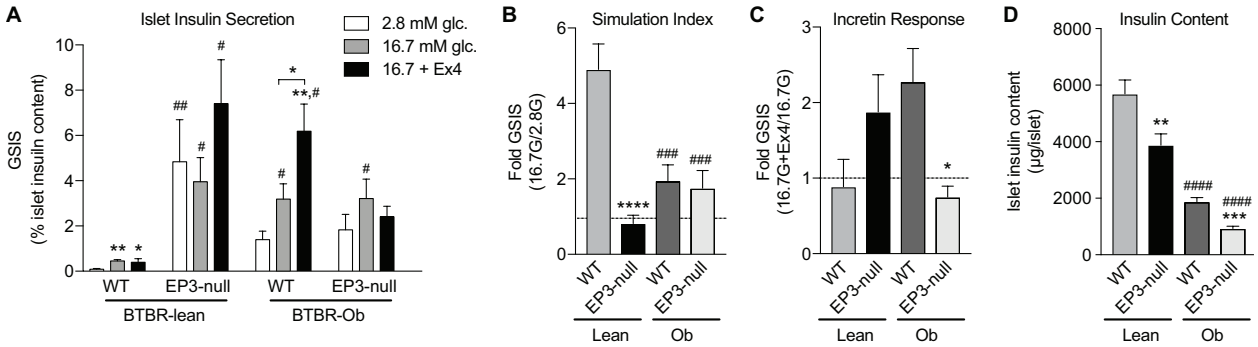

Figure 4: Pancreatic islets from EP3-null mice have a dysfunctional insulin secretion response. A: Glucose-stimulated insulin secretion (GSIS) as a percent of content in response to 2.8 mM glucose (low), 16.7 mM glucose (high) or 16.7 mM glucose with 10 nM exendin-4 (Ex4). B: Islet stimulation index, or GSIS in 16.7 mM glucose normalized to that in 2.8 mM glucose. C: Islet incretin response, or GSIS in 16.7 mM glucose + Ex4 normalized to that in 16.7 mM glucose alone. D: Mean islet insulin content. In (A), within-group data analysis (groups: BTBR-lean and BTBR-Ob) was performed by one-way ANOVA with Holm-Sidak test post-hoc to correct for multiple comparisons. *, $p < 0.05$ and **, $p < 0.01$ vs. insulin secreted in 2.8 mM glucose. $^{\#}$, $p < 0.05$ and $^{\#\#}$, $p < 0.01$ vs. the same stimulation condition in WT lean islets. In (B), (C), and (D), data were compared within and among groups by two-way t-test. **, $p < 0.01$, ***, $p < 0.001$, and ****, $p < 0.0001$ vs WT lean or WT Ob. $^{\#}$, $p < 0.05$, $^{\#\#\#}$, $p < 0.001$, and $^{\#\#\#}$, $p < 0.0001$ vs. WT lean or EP3-null lean. In A-C, $N \geq 5$ independent measurements. In D, $N \geq 32$ independent measurements. In all panels, if a comparison is not indicated, the difference in means was not statistically significant.

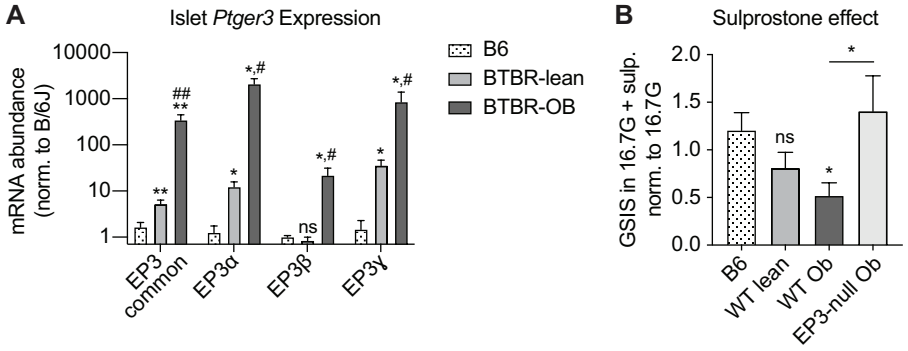

Figure 5. Total EP3 mRNA and EP3γ splice variant mRNA abundance are differentially expressed in isolated islets by strain background and T2D status. A: qPCR analyses of islet cDNA samples from C57BL/6J (B6), BTBR-lean, and BTBR-Ob mice for total EP3 mRNA or mRNA encoding individual splice variants. B: GSIS in 16.7 mM glucose with 10 nM sulprostone normalized to that in 16.7 mM glucose alone. In both panels, within-group data analysis (groups: B6, BTBR-lean and BTBR-Ob) was performed by one-way ANOVA with Holm-Sidak test post-hoc to correct for multiple comparisons. *, $p < 0.05$ and **, $p < 0.01$ vs. B6; and $^{\#}$, $p < 0.05$ and $^{\#\#}$, $p < 0.01$ vs. BTBR-lean. In (B), data were compared by one-way ANOVA with Holm-Sidak test post-hoc to correct for multiple comparisons. *, $p < 0.05$ vs. B6 lean or the indicated comparison. In both panels, N=3-10 independent measurements per group, and if a comparison is not indicated, the difference in means was not statistically significant.